Ecological Informatics 69 (2022) 101658

Contents lists available at ScienceDirect

Ecological Informatics

journal homepage: www.elsevier.com/locate/ecolinf

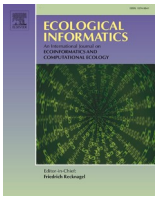

Estimating boreal forest ground cover vegetation composition from nadir photographs using deep convolutional neural networks

Hilary A. Cameron [a], Pranoy Panda [b], Martin Barczyk [c], Jennifer L. Beverly [a,*]

[a] Department of Renewable Resources, University of Alberta, Edmonton, AB T6G 2H1, Canada
[b] Department of Computer Science and Engineering, IIT Hyderabad, Sangareddy, Telangana 502285, India
[c] Department of Mechanical Engineering, University of Alberta, Edmonton, AB T6G 1H9, Canada

A B S T R A C T

Ground cover and surface vegetation information are key inputs to wildfire propagation models and are important indicators of ecosystem health. Often these variables are approximated using visual estimation by trained professionals but the results are prone to bias and error. This study analyzed the viability of using nadir or downward photos from smartphones (iPhone 7) to provide quantitative ground cover and biomass loading estimates. Good correlations were found between field measured values and pixel counts from manually segmented photos delineating a pre-defined set of 10 discrete cover types. Although promising, segmenting photos manually was labor intensive and therefore costly. We explored the viability of using a trained deep convolutional neural network (DCNN) to perform image segmentation automatically. The DCNN was able to segment nadir images with 95% accuracy when compared with manually delineated photos. To validate the flexibility and robustness of the automated image segmentation algorithm, we applied it to an independent dataset of nadir photographs captured at a different study site with similar surface vegetation characteristics to the training site with promising results.

1. Introduction

Surface vegetation is a key indicator of ecosystem health. The percent of ground surface covered by vegetation and biomass loadings are common descriptors used to characterize ecosystems (Houghton et al., 2009; Spurr and Barnes, 1973). Quantitative descriptions of ground cover and surface vegetation have been used to evaluate habitat suitability (e.g., Etchberger et al., 1989), predict the likelihood of flooding events (e.g., Michener and Houhoulis, 1997), explain observed wildfire behaviour (e.g. Thompson et al., 2020), determine rangeland health conditions (e.g., Pyke et al., 2002), and predict how climate change may alter forest structure and composition (e.g., Whitman et al., 2019). Despite the importance of these measurements, development of rapid and effective field measuring techniques for ground cover in forested environments has received little attention.

In forested areas, ground cover and surface vegetation data are typically collected in-situ by field crews using laborious sampling protocols, which are both time consuming and costly (Sikkink and Keane, 2008). Traditionally, field plots are established and line intercept or fixed area sampling techniques are conducted to document the characteristics of the site (Sikkink and Keane, 2008). The resulting measurements are accurate (Booth et al., 2006; Keane and Gray, 2013), but a single plot can take hours to thoroughly document. Rapid, non-destructive approaches have evolved to replace traditional field methods and include ocular estimation in which a trained professional estimates ground cover visually. The accuracy of visual assessment is relatively poor (±10–20%, Hahn and Scheuring, 2003) and vulnerable to inconsistencies among observers (Sykes et al., 1983). Kennedy and Addison (1987) found that visual estimates can have error rates >51% and are especially high for low cover classes.

Additional forest floor descriptors, such as biomass loadings of litter, lichen or dead and down material, are important measurements for understanding potential wildfire behaviour (Graham et al., 2004). The arrangement, loading, composition, and condition of combustible material on the forest floor will directly affect surface wildfire intensity (Graham et al., 2004) and the probability of ignition is known to vary by surface fuel type (Beverly and Wotton, 2007). Visual estimation has been used extensively to rapidly assess surface fuel loads in support of forest fire management. Keane and Dickinson, 2007 developed a set of photographs for visually estimating fuel loads and these have been used in operational field settings, where field inventories are impractical. Although fast and inexpensive, ocular fuel load estimates require trained field personnel to interpret photographs and the resulting estimates are considered less accurate than planar intercept and fixed-area microplot measurements (Keane and Gray, 2013). For Australian eucalypt forests, Volkova et al. (2016) reported that visual assessments of fuel loads

* Corresponding author.
E-mail address: jen.beverly@ualberta.ca (J.L. Beverly).

https://doi.org/10.1016/j.ecoinf.2022.101658
Received 4 May 2021; Received in revised form 26 April 2022; Accepted 26 April 2022
Available online 5 May 2022

performed poorly relative to destructively sampled fuel load values, with errors ranging from −50% to 200%.

Smartphone applications (apps) have also been developed to collect ground-based observations of forest structures (e.g. Ferster et al., 2013). Due to their broad availability and ease of use, smartphone applications are well-suited for enlisting the public in scientific research (i.e., citizen science), which can enable data collection at temporal and spatial scales that would be impractically lengthy and cost-prohibitive for traditional field research studies. Smartphones are equipped with high-resolution cameras, global positioning system (GPS) receivers, photo-location geotagging services, and have the ability to store and transfer data easily making them an ideal tool to collect and aggregate information. Ferster and Coops (2014) used both professionals and non-professionals to gather forest inventory data using a smartphone app to estimate forest fuels. In that study, the user input coarse, visual estimates of percent coverage of large woody debris, fine woody debris and flammable surface vegetation. Significant differences between estimates recorded by professionals and non-professionals were reported, demonstrating that users would require training to ensure consistent results, which undermines the intended function of rapid data collection methods for broad use by non-specialists in opportunistic situations. Other apps such as Trestima (Rouvinen, 2014), Canopeo (Patrignani and Ochsner, 2015), and MOTI (Rosset et al., 2014) have been designed to capture forest structure information automatically but are limited to forest canopy measurement or ground cover measurement in grassland or agricultural settings (e.g. Vastaranta et al., 2015).

In recent years, computer algorithms have emerged as a promising alternative for transforming photographs into data documenting real-world features (e.g. Van Horn et al., 2018) while also eliminating the variability associated with photo-interpretation by humans. One of the most basic forest floor attributes that can be extracted from nadir or downward photos is the percent cover of different ground cover classes. Models that perform automatic image segmentation to estimate percent ground cover using downward-facing digital photographs have reported promising results (e.g. Abdalla et al., 2019; Yu and Guo, 2021); however, most of this work has been conducted in agriculture or grassland environments with characteristically uniform ground cover morphologies (e.g. McCool et al., 2018), and few studies have attempted photo-based measurement of the more complex and heterogenous ground cover environments characteristic of forest ecosystems.

The accuracy of computer-based nadir photo interpretation is typically evaluated by comparing results to photo-interpretation by a trained ecologist (e.g. Booth et al., 2005; Luscier et al., 2006). Regardless of whether a computer or an ecologist interprets a nadir ground cover photo, the results will be affected by visual occlusion due to some vegetation types obscuring the vegetation beneath. In agricultural field and grassland environments, vertical overlap of different vegetation types may be minimal; however, in forested environments, nadir photographs are expected to omit occluded ground cover that would have been visible during an in-situ field assessment (Duan et al., 2017; Morrison, 2016).

Ground cover estimation from images taken in forested environments is complicated not only by the highly heterogenous vegetation conditions, but also by the varied lighting conditions which can hinder computer algorithms developed to process the digital images (Chianucci, 2020; Macfarlane and Ogden, 2012). Macfarlane and Ogden (2012) developed one of the first algorithms for predicting total understory (i.e., all surface vegetation) cover from nadir images. Song et al. (2015) and Salas-Aguilar et al. (2017) proposed new methods to quantify total understory vegetation cover in shady, agricultural and forested environments. In these studies, no attempt was made to differentiate between vegetation types, so occlusion was not a concern. Despite promising early results, few attempts have been made to estimate vegetative cover in forested environments with nadir photographs (Chianucci, 2020) and to our knowledge, no attempts have been made to classify ground cover composition in forested stands into vegetation subtypes such as moss, forbs, grass, or shrub cover.

Quantifying forest surface coverage by type with nadir photographs could have profound implications for wildfire behaviour modelling (e.g., de Groot, 2012; Linn, 1997) and a wide range of ecological studies (e.g., Booth et al., 2006; Brewer, 2016) that rely on accurate ground cover and vegetative information. To date, most investigations of vegetation cover estimation from nadir photography have used carefully controlled image capture protocols combined with professional grade photographic equipment. Large-scale collection of nadir photographs to document vegetation cover in operational field settings requires development of alternative image capture protocols based on accessible, low-cost equipment and less restrictive procedures. Consumer grade photographic equipment has been used to adequately measure ground cover in agricultural environments (e.g. McCool et al., 2018) but has yet to be tested in more complex vegetation settings. Rigid protocols and supplementary equipment, such as extendable poles (e.g. Macfarlane and Ogden, 2012) and tripods (e.g. Abdalla et al., 2019) that raise and level the camera; or the precondition for overcast lighting during photo acquisition (Macfarlane and Ogden, 2012) limit the ability to collect data broadly and quickly. Using nadir photography for large scale collection of ground cover and surface vegetation by the public, field personnel, or with autonomous systems such as aerial drones or wheeled robots requires development and testing of flexible photo acquisition protocols using inexpensive and ubiquitous consumer grade smartphone cameras.

This study aims to assess the viability of using consumer-grade smartphone cameras combined with flexible photo acquisition protocols to accurately describe basic ground cover and surface vegetation composition in forested stands. We evaluate performance of both manually interpreted nadir photographs and a machine learning-based image segmentation algorithm to explore the viability of automating estimation of ground cover and biomass loadings from nadir images. Nadir photographs taken at field sites in forested stands in Alberta, Canada, were paired with field measurements of ground cover and above-ground biomass inventoried by trained crews following standard protocols for documenting forest fuels relevant to wildfires. Correlations between field measurements and manually interpreted photo data were assessed. Manually interpreted photo data were used to train a deep convolutional neural network (DCNN)-based semantic segmentation algorithm, which assigns vegetation type labels to every pixel in the image. Finally, the resulting trained network was applied to an independent set of photographs collected at a different field site to evaluate performance relative to in-situ field measurements.

2. Methods

2.1. Study sites

Nadir photographs and field measurements of ground biomass were collected simultaneously at 32 field plots during summer conditions (July–August) over the 2018 and 2019 field seasons. Measurement plots were located at three different field sites in the Boreal Forest Natural Region of central Alberta (Fig. 1): Pelican Mountain (PM, $n = 20$), Calling Lake (CL, $n = 3$) and Conklin (CK, $n = 9$). Plots established at PM and CL were used to train and test the semantic segmentation model, while plots established at CK were used solely for independent validation. These three sites were selected for ease of access and to ensure the range of surface vegetation cover types included in the study were representative of boreal forest ecosystems. Plots used for training and testing the semantic segmentation model included pure, natural black spruce (*Picea mariana*) stands ($n = 8$), pure, managed black spruce stands (n = 2), mixed black spruce and larch (*Larix laricina*) stands ($n = 5$), and recently burned pure black spruce stands (n = 8). Plots used for independent validation included natural black spruce dominated stands (n = 2), managed black spruce dominated stands ($n = 4$), and managed jack pine (*Pinus banksiana*) dominated stands (n = 3). A schematic

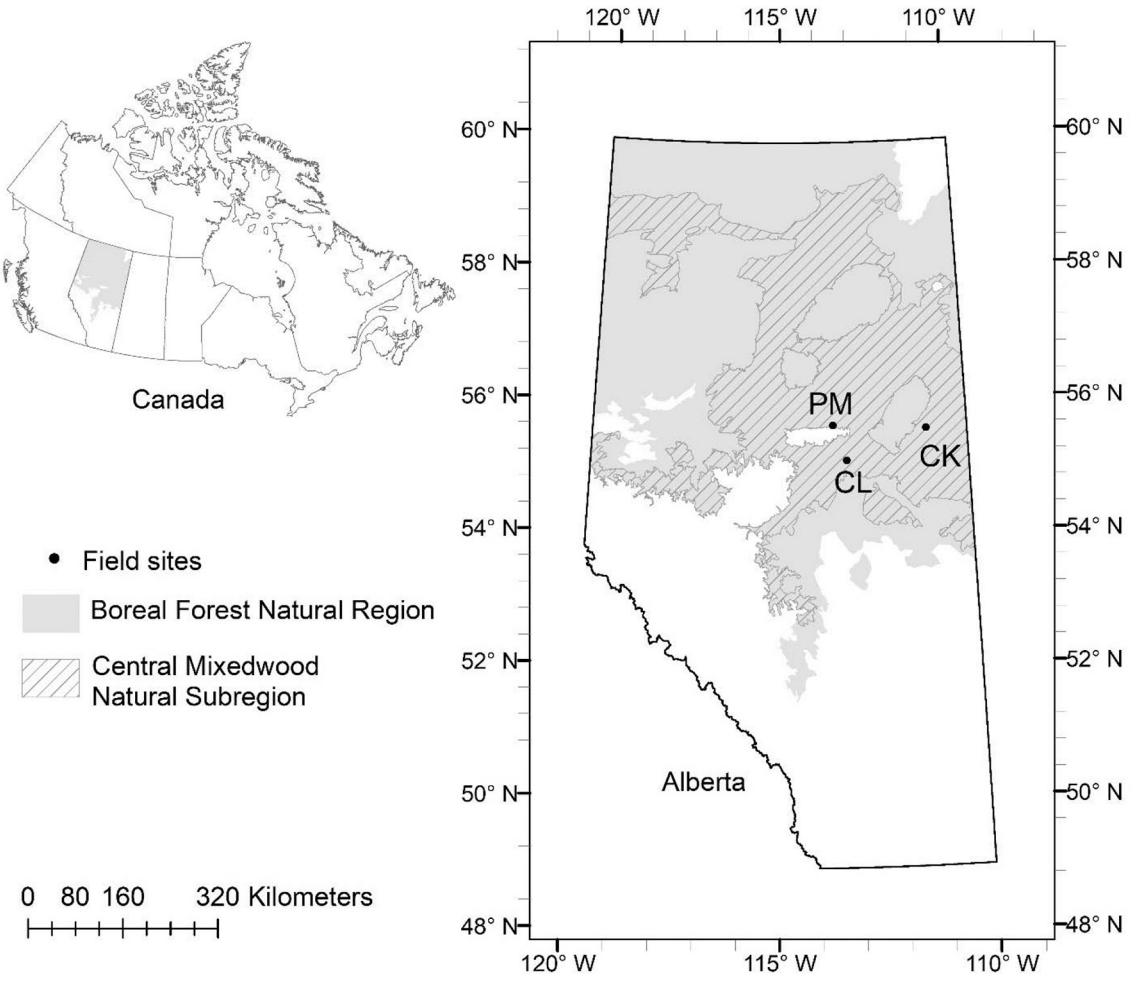

Fig. 1. Field site locations in the province of Alberta, Canada. Data collected at Pelican Mountain (PM) and Calling Lake (CL) were used for training and testing the deep convolutional neural network (DCNN) semantic segmentation algorithm. Data collected at Conklin (CK) were used solely for independent validation.

overview of the methodological steps taken and associated datasets used at each step is shown in Fig. 2.

2.2. Ground photographs

At each plot, two 50 m perpendicular lines were established. One line was oriented north-south and the other east-west, such that they bisected each other to form four 25 m transects in each of the four cardinal directions emanating from the plot centre. Along each transect, downward photographs were acquired at 5 m intervals beginning at 5 m from plot centre. Images were taken with an Apple iPhone 7 smartphone using the primary lens on the back of the camera with a 12MP resolution, f/1.8 aperture, and optical image stabilization. During photo acquisition, the camera was positioned at arm's length from the photographer and hand-leveled horizontally at waist height approximately 1 m above the ground. The camera's digital screen included a leveling feature to assist with hand-leveling.

The 5 m spacing between photos ensured that images were independent and did not overlap. The precise area captured in each image was influenced by small variations in the height of the camera above the forest surface caused by undulating terrain within and between plots as well as differences in the heights of the photographers, but we do not expect this to influence results which were based on proportions rather than area. In general, the area contained in each photo approached 0.81 m^2 which corresponds to 0.25 mm pixels with photos spaced 20,000 pixels apart.

2.3. Field measurements

Percent ground cover was estimated from field measurements using the point intercept method (Bonham, 1989). At 0.5 m intervals along each transect, field crews recorded ground cover directly under the transect by noting the presence of six possible ground cover types: forbs, grass, lichen, feather moss, sphagnum moss, or other moss. For each ground cover type, percent cover was calculated as the total number of observed instances of the ground cover type (i.e., "hits") divided by the maximum possible number of hits (i.e., 200).

Biomass loadings important to surface fire behaviour were also collected for four different fuel categories: fine woody debris (FWD), shrubs, herbaceous fuels (grass and forbs), and litter. Woody debris was defined as twigs, limbs, branches, smaller stems, and large logs at a 45 degree angle to the ground or less (Brown, 1974; Van Wagner, 1968). Fine woody debris consists of wood pieces with diameter $\leq$ 7.0 cm and were assessed by size class following McRae et al. (1979) : 0.0–0.5 cm (class 1), 0.6–1.0 cm (class 2), 1.1–3.0 cm (class 3), and 3.1–5.0 cm (class 4) and 5.1–7.0 cm (class 5).

The planar intercept method was used to calculate FWD fuel loads. This method was originally developed by Warren and Olsen (1964) and revised by Brown (1974) to expedite field measurements and is widely used to estimate the fuel load of dead and down woody material (e.g. Lutes et al., 2005). The number of FWD pieces by size class were tallied along each transect. To reduce measurement time and avoid redundancy, the length of transects used for measurement varied by FWD size class: 5 m (class 1), 10 m (class 2), 15 m (class 3), 20 m (class 4), and 25

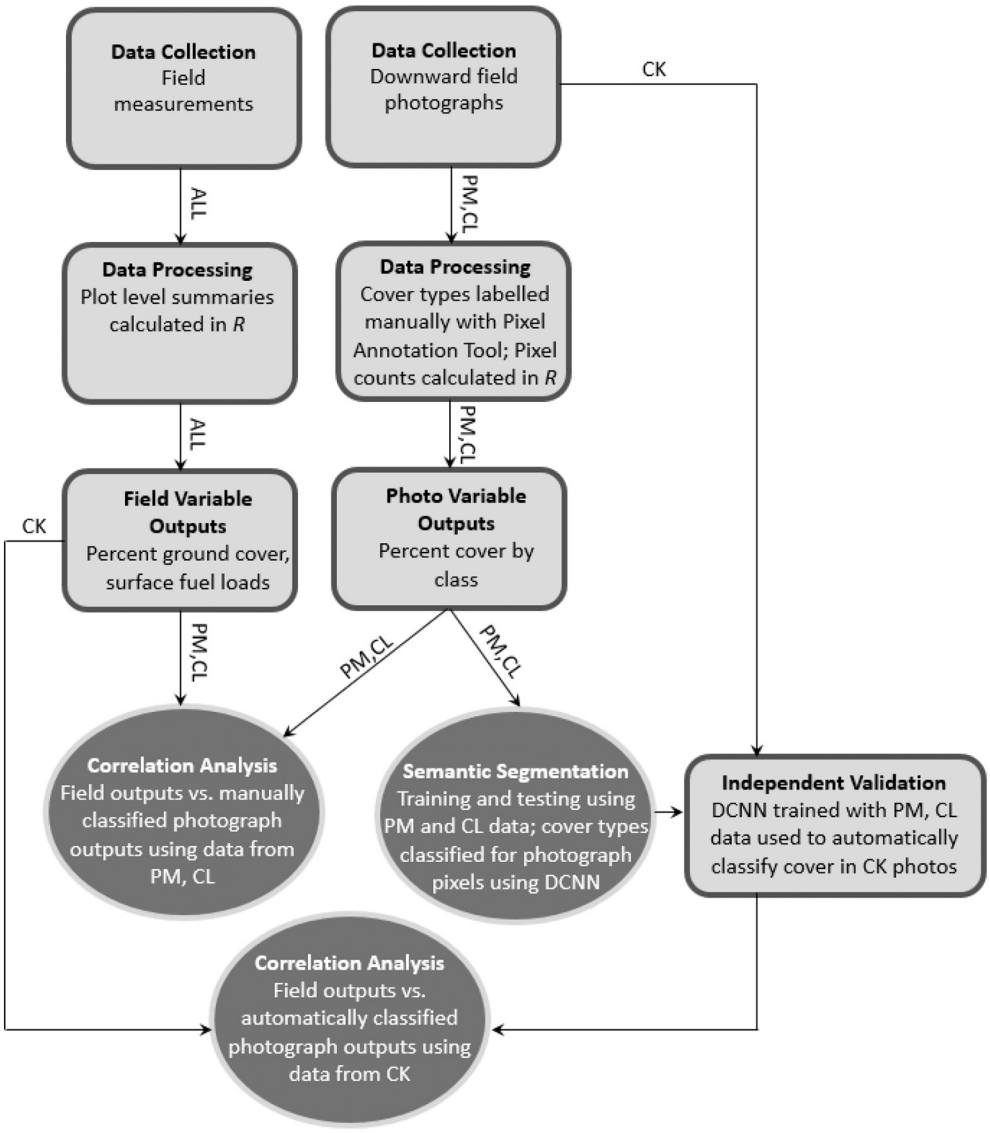

Fig. 2. Schematic diagram of methodological steps. Field measurements were collected at three field sites: Pelican Mountain (PM), Calling Lake (CL) and Conklin (CK). Manual classification of fuel types used in semantic segmentation training and testing were limited to data collected at PM and CL. Field measurement data and raw photos from the CK field site were used solely for independent validation. R refers to the R programming language and environment for statistical computing (R Core Team, 2020). DCNN refers to deep convolutional neural network.

m (class 5). Overstory composition for each transect was estimated for up to two species. Fuel load for each FWD size class was calculated by transect using the following formula:

$$W_{fwd} = \left(\left[\frac{\pi^2\, G_1 sec(h) n\, QMD^2\, c}{8L}\right] \times S_1\right) + \left(\left[\frac{\pi^2\, G_2 sec(h) n\, QMD^2\, c}{8L}\right] \times S_2\right) \quad (1)$$

where W_{fwd} is the fuel load for the given size class (Mg ha^{-1}), h is the piece tilt angle (degrees), n is the number of intercepts (i.e. hits) along the length of the transect (L, m), QMD is the quadratic mean diameter (cm), c is the slope correction factor (equal to one given that all sites were flat), G_x is the specific gravity for species x (g cm^{-3}), and S_x is the percent overstory composition estimated by field crews for species x. Values from Nalder et al. (1999) were used for h and QMD. Values for G were obtained from the sources listed in Table 1. Fuel load calculated for each size class was summed per transect and then averaged across all transects to provide a plot-level estimate of FWD fuel load.

Shrub cover by transect was measured using the planar intercept method and average height was recorded. Shrub fuel load was calculated by transect and species using the generalized formula reported by Olson and Martin (1981):

Table 1
Sources of specific gravity by species type we to calculate fuel load of dead and down material in this study.

Species	Specific gravity reference
Engelmann Spruce (*Picea engelmannii*)	Bessie and Johnson (1995)
Lodgepole Pine (*Pinus contorta*)	
Trembling Aspen (*Populus tremuloides*)	
White Spruce (*Picea glauca*)	Delisle and Woodard (1988)
Douglas Fir (*Pseudotsuga menziesii*)	
Black Spruce (*Picea Mariana*)	Nalder et al. (1999)
Jack Pine (*Pinus banksiana*)	
Larch (*Larix laricina*)	

$$W_{shrub} = ((0.0577 \times \%cover \times height) - 0.62689) \times 0.002 \quad (2)$$

where W_{shrub} is the shrub fuel load (kg m^{-2}), height is the average shrub height along the transect (cm), and 0.002 is a conversion factor. Shrub fuel load by plot was calculated as the average of transect fuel loads.

Herbaceous fuel load was calculated using destructive samples 1 m^2 in size and positioned at the end of each transect (Fig. 3). All grass and forbs present in the sample area were clipped to ground level, removed from the site and oven-dried at 105 °C for 24 h. Sample weights were

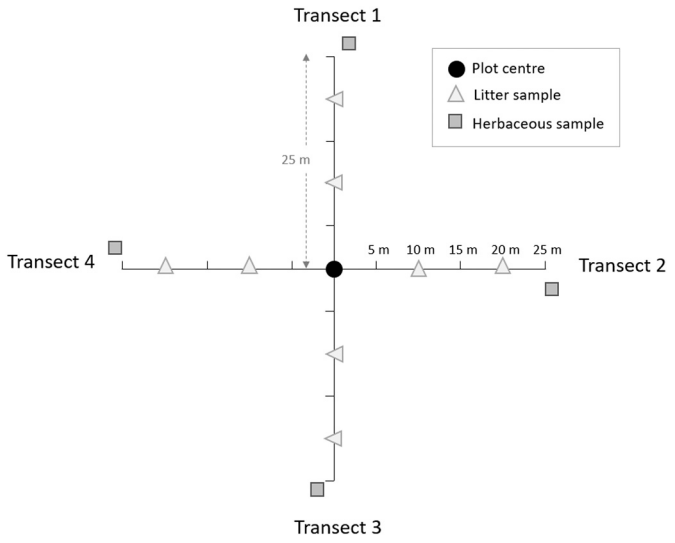

Fig. 3. Field plot layout and configuration of litter and herbaceous destructive samples used to compute fuel loads.

averaged to estimate herbaceous fuel load (kg m^{-2}) by plot. Litter fuel load was estimated with 0.01 m^2 destructive samples at 10 m and 20 m on each transect, measured from plot centre. Within the destructively sampled area, all litter biomass extending from the ground to the duff layer was collected and oven-dried. Litter samples included moss, fallen foliage and lichen fuels and were averaged by plot. Other fuel types within the sample area were removed, including grass, shrubs, and woody material. Herbaceous and litter fuel load was calculated as:

$$W_{herb} = \frac{M}{A} \tag{3}$$

where W_{herb} is the fuel load of the sample (kg m^{-2}), M is the mass of the sample collected (kg), and A is the sample area (m^{-2}).

2.4. Manual photo processing

Photographs acquired at PM and CL sites were manually labeled with the Pixel Annotation Tool (Breheret, 2017). Manual annotations consisted of ten possible cover types: woody debris, shrub, forb, grass, lichen, feather moss, sphagnum moss, other moss, non-fuel (e.g. water, soil, rock), and void, which was assigned to pixels that did not belong to any other cover types. Portions of the photo were sometimes left unclassified due to time constraints, for example due to extremely fine patterns of multiple cover types within very limited spatial areas. Photos with ≥15% unclassified pixels were omitted, resulting in a final set of 330 photos retained for analysis. Pixel counts by cover type were calculated for each photo in R (R Core Team, 2020) using the png package (Urbanek, 2013). Percent ground cover composition for forbs, grass, lichen, feather moss, and sphagnum moss categories were calculated in relation to the combined area of the photo assigned to these ground cover types. Areas labeled as shrub were omitted from ground cover calculations because they effectively obscured ground cover underneath. Percent cover of woody debris, shrub, herbaceous fuel (forbs and grass), and litter (mosses and lichen) were calculated using all pixel totals. Correlations between photo-based percent cover and field measurements of ground cover or fuel loads were evaluated in R using the ggplot2 package (Wickham, 2016). Manually classified photos were randomly divided into training ($n = 290$) and testing ($n = 40$) groups for semantic segmentation.

Drawing training and testing data from the same plot locations has the potential to introduce spatial autocorrelation. For any spatially referenced ecological data, nearby locations can be expected to be more similar than distant ones (Tobler, 1970). The standard solution is to place samples sufficiently apart from one another. Unfortunately, to ensure test data had ecological conditions representative of the training data, it was necessary to draw these data from the same plots as the training data. We considered this approach acceptable in our case because the forest floor conditions in our plots were heterogenous over very small distances (i.e., millimeters to centimeters) and photos spaced just 5 m apart could have very different proportionate representations of cover types. Given the area included in each training and testing photo was completely independent and the distance between photos was relatively large (i.e., 20,000 pixels), we expect spatial autocorrelation between training and testing data likely was minimal.

2.5. Semantic segmentation

The goal of semantic segmentation is to automatically assign one of the ten previously described cover types to each pixel of the nadir image. This is a complex task since many vegetation types have only subtle differences in appearance, and exhibit irregular shapes and sizes. We used the framework of deep convolutional neural networks (DCNN) in our work as it has been found to work well for semantic segmentation purposes; however, this framework is notorious for requiring a large number of labeled images for the training process, which we lacked. Therefore, we opted to use Transfer Learning when dealing with our limited dataset. Transfer learning involves transferring knowledge acquired by training a model in one particular task to another, related task.

In our case, we used the pre-trained Deeplabv3-ResNet101 model (Chen et al., 2017) as our base network for deriving knowledge to solve our current task. This base network has been trained on a subset of the COCO train2017 dataset (Lin et al., 2015), consisting of a few thousand images, using the 20 categories present in the Pascal VOC dataset (Everingham et al., 2010). The transfer learning methodology used in our work is shown in Fig. 4. Our deep convolutional neural network uses the convolution layers of the Deeplabv3-Resnet101 network as a learned feature extractor. We then attached a classification head of 2048 neurons with sigmoid activation. Therefore, each pixel was assigned 10 scores in the range of 0 to 1, for the 10 classes, and the class with the highest score was declared as the predicted class for that pixel. We used the cross-entropy loss as the objective function for training our network, and the Adam (Kingma and Ba, 2014) optimizer for updating the trainable parameters.

Since the multi-class (i.e. 10 classes) semantic segmentation problem is quite complex, the set of 290 training images was found to be insufficient to obtain satisfactory results, even with the use of the transfer learning framework. Therefore, we employed data augmentation strategies to increase the training set size fourfold: horizontal flip, Gaussian noise addition, and contrast reduction. The first two augmentation strategies are fairly common. The contrast reduction strategy was specifically motivated by our application, namely given that we expect the images to contain shadows occluding the vegetation types, contrast reduction helps to simulate areas of low lighting which can be expected in the dataset.

Further, in general, datasets generated from natural scenes for semantic segmentation have significant variation in the occurrence frequencies of different classes. To address this, we used median frequency balancing to weight the loss based on the correct label/class, where the weight given to each class in the loss function is the ratio of the median of class frequencies over the entire dataset divided by the class frequency (Eigen and Fergus, 2015).

2.6. Testing and independent validation

The deep convolutional neural network was tested using 40 of the manually classified photos collected at PM and CL field sites that were withheld from training. The algorithm was then subjected to an independent validation exercise in which it was applied to a set of photos

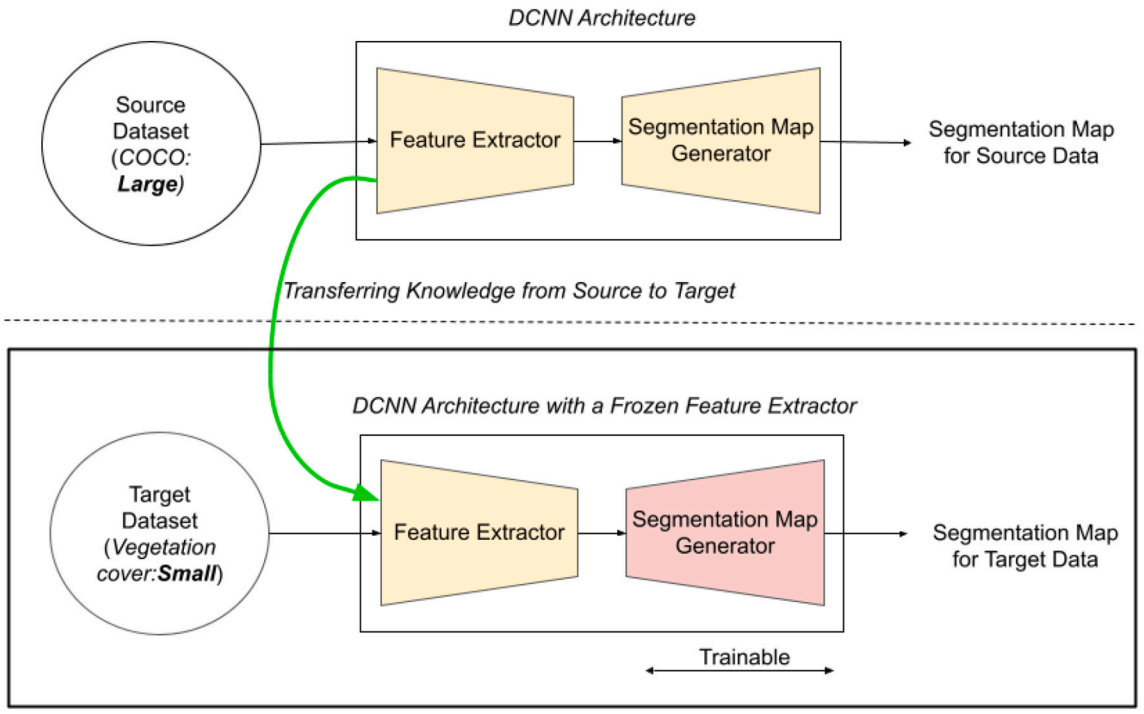

Fig. 4. Transfer Learning methodology for training our network.

acquired at the CK field site, which were not used in either the manual comparisons with field data or the deep convolutional neural network model training. Correlations between the automatically segmented photos and field measured data from the CK field site were undertaken with the same methods described previously for the manually segmented photos collected at the PM and CL field sites.

3. Results

3.1. Relationship between manual image classification and field measured variables

All three field sites (i.e., PM, CL, CK) had similar characteristics despite their different geographic locations (Table 2). Litter and feather moss were the dominant ground cover types and surface vegetation was mainly composed of Labrador tea (*Ledum groenlandicum*), lowbush cranberry (*Vaccinium vitis-idaea*), blueberry (*Vaccinium myrtilloides*) and bog cranberry (*Vaccinium oxycoccos*). Most sites had an organic layer over 40 cm in depth and minimal downed woody debris. Due to time constraints, herbaceous and litter samples were omitted at the validation site (CK, $n = 9$). Overall, sites had low fine woody debris, herbaceous and shrub fuel loads with moderate litter fuel loads.

Removal of photos with >15% unclassified pixels reduced the number of photos available for analysis to between 10 and 20 manually segmented photos per plot. Relationships between percent cover of a given pixel type by plot and corresponding field measured percent cover of forbs, grasses, lichen, feather moss, and sphagnum moss are shown in Fig. 5. None of the cover types exhibited a strong 1:1 correlation between field measured values and photograph pixel composition, which was expected given the known omission of occluded vegetation in the photos. The relatively strong Pearson's correlation coefficient (r) values for the forb (0.69), lichen (0.69) and sphagnum moss (0.88) classes are influenced by the uneven data distribution and presence of outliers; however, field-measured grass and feather moss percent cover was strongly correlated with percent cover estimated manually from the photographs, with r values of 0.85 and 0.91, respectively. In general, recently burned plots had lower percent cover values for all cover types than natural or thinned stands which allowed for a larger range of ground cover values to be captured. All comparisons between manually derived ground cover composition and field-measured values produced significant (p-value <0.05), positive correlations (Table 2).

Relationships between percent cover of a given pixel type and corresponding field measured fuel loads for FWD, shrub, herbaceous and

Table 2
Physical characteristics of the three field sites: Pelican Mountain (PM), Calling Lake (CL) and Conklin (CK).

Physical characteristic	Field Site		
	PM	CL	CK
Latitude, longitude, degrees	55.7008, −113.5689	55.2103, −113.1933	55.6319, −111.0843
Area, km^2	1.5	6	7.5
Date of data collection	July–August 2019	July–August 2019	August 2018
Number of plots	20	3	9
Primary tree species composition	Black spruce, larch	Black spruce	Black spruce, jack pine
Dominant ground cover type (number of plots)	Litter (10), feather moss (8), sphagnum moss (1), grass (1)	Feather moss (3)	Litter (3), sphagnum moss (3), feather moss (2), grass (1)
FWD fuel load range (average), kg m^{-2}	0.02–0.43 (0.17)	0.18–0.55 (0.34)	0.05–0.71 (0.25)
Shrub fuel load range (average), kg m^{-2}	0.00–0.47 (0.13)	0.05–0.20 (0.13)	0.02–0.27 (0.12)
Herbaceous fuel load range (average), kg m^{-2}	0.00–0.015 (0.003)	0.00–0.003 (0.002)	NA
Litter fuel load range (average), kg m^{-2}	0.00–0.6 (0.30)	0.62–0.8 (0.69)	NA

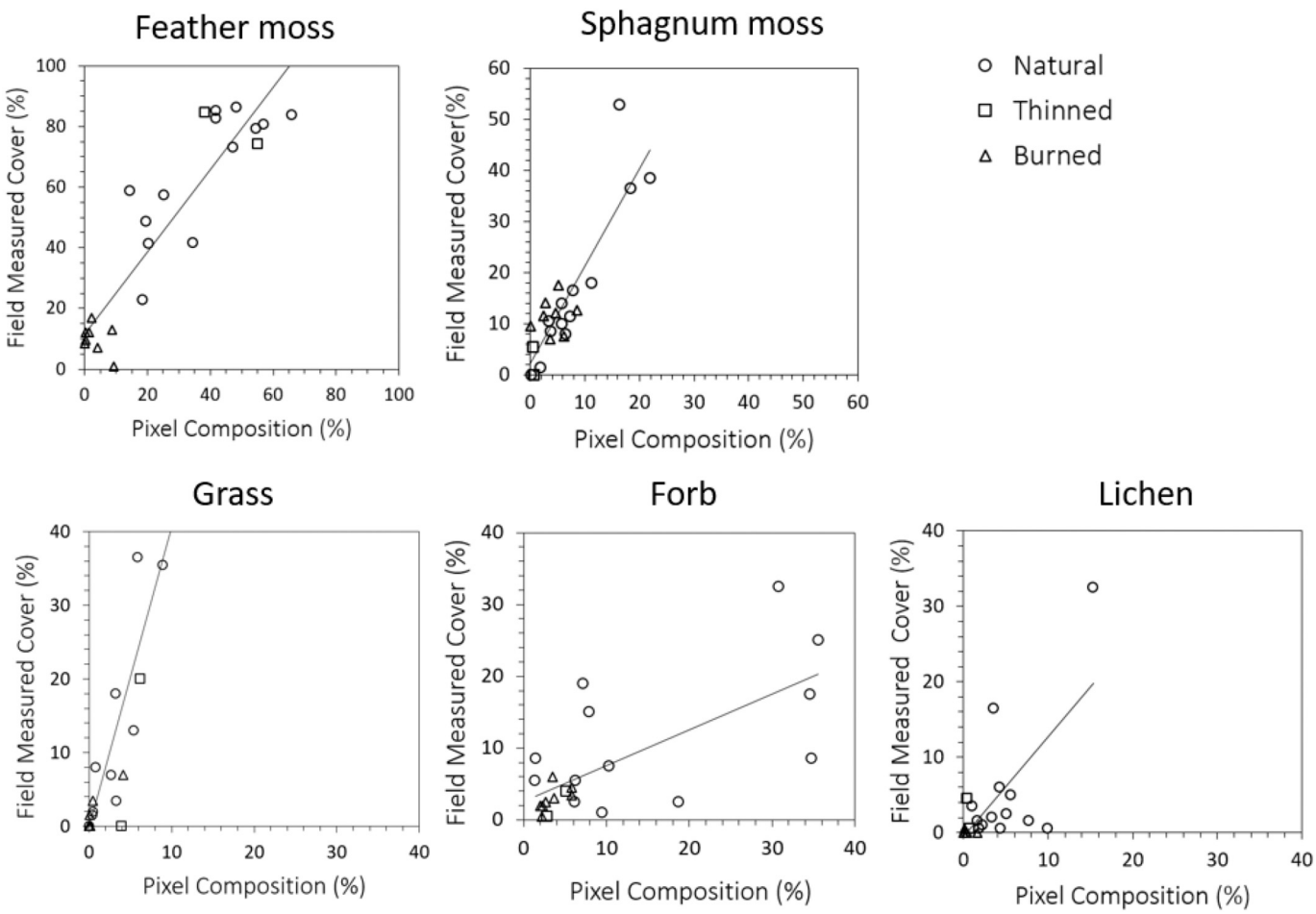

Fig. 5. Relationship between field-measured percent ground cover and percent cover from pixel composition of manually segmented photos at Pelican Mountain (PM) and Calling Lake (CL) plots, shown for each cover type: feather moss, sphagnum moss, grass, forb, and lichen.

litter categories are shown in Fig. 6. Unsurprisingly, photo-based estimates of percent cover, which by their nature do not render the three-dimensional aspect of fuels, were at best weakly correlated (r = 0.42–0.77) with fuel load measurements.

3.2. Semantic segmentation validation

The semantic segmentation deep convolutional neural network trained using the manually segmented nadir images from PM and CL field sites was evaluated on 40 images reserved for testing, using two standard metrics from computer vision: mean intersection over union (mIoU), which is the proportion of overlap between the manually segmented photo and the prediction output; and accuracy, which is calculated as the proportion of pixels in the image that were correctly classified. We obtained an overall mIoU of 0.352, a rather low value, but an accuracy of 0.95, indicating that 95% of the pixels were classified correctly and that our trained model accurately predicts the prominent vegetation classes in individual images. A low mIoU value can be misleading since it assigns equal weights to every type of ground cover, irrespective of its proportion in an image. Table 3 shows the same performance metrics by class for the test data. For each image, we only considered cover types that occupied at least 1% of the manually classified segmentation map. In most cases, the class result approaches the average, but some classes such as lichen and 'other moss' had notably low mIoU values, which is not surprising given the low frequency of occurrence of these classes.

Samples of raw nadir field photos in our validation dataset, their manual semantic segmentation by a human expert (observed) and automatic semantic segmentation by our DCNN (predicted) are shown in Fig. 7. Visual inspection of the images suggests there is good correspondence between observed and predicted ground cover classes.

3.3. Semantic segmentation algorithm outputs comparison with field-based measurements

The DCNN-based semantic segmentation algorithm trained with photos acquired at PM and CL field sites was applied to photos acquired at plots (n = 9) located at the CK field site, to test the flexibility and robustness of the algorithm. The correlations by cover type (forbs, grass, lichen, feather moss and sphagnum moss) are shown in Fig. 8. A very strong correlation was observed for grass (0.96), but one data point with a high field-measured grass value likely influenced the strength of this relationship. Correlations for forb, lichen, feather and sphagnum ground covers ranged from 0.58 to 0.75. Lichen was the only ground cover type to have an insignificant relationship (p-value >0.05) between field measurements and automatic semantic segmentation results (Table 4).

Field measured fine woody debris (FWD) and shrub fuel loads from Conklin were also compared with average corresponding pixel composition in the automatically segmented photos (Fig. 9). Herbaceous and litter fuel loads were not collected at Conklin due to time constraints and were therefore not analyzed. A weak correlation (r = 0.5) was observed between fine woody debris fuel loads and woody debris percent ground cover derived from automatically segmented images. There was almost no correlation (r = 0.02) between field measured shrub fuel loads and the shrub percent ground cover derived from automatically segmented images. Neither correlation was found to be significant (Table 5).

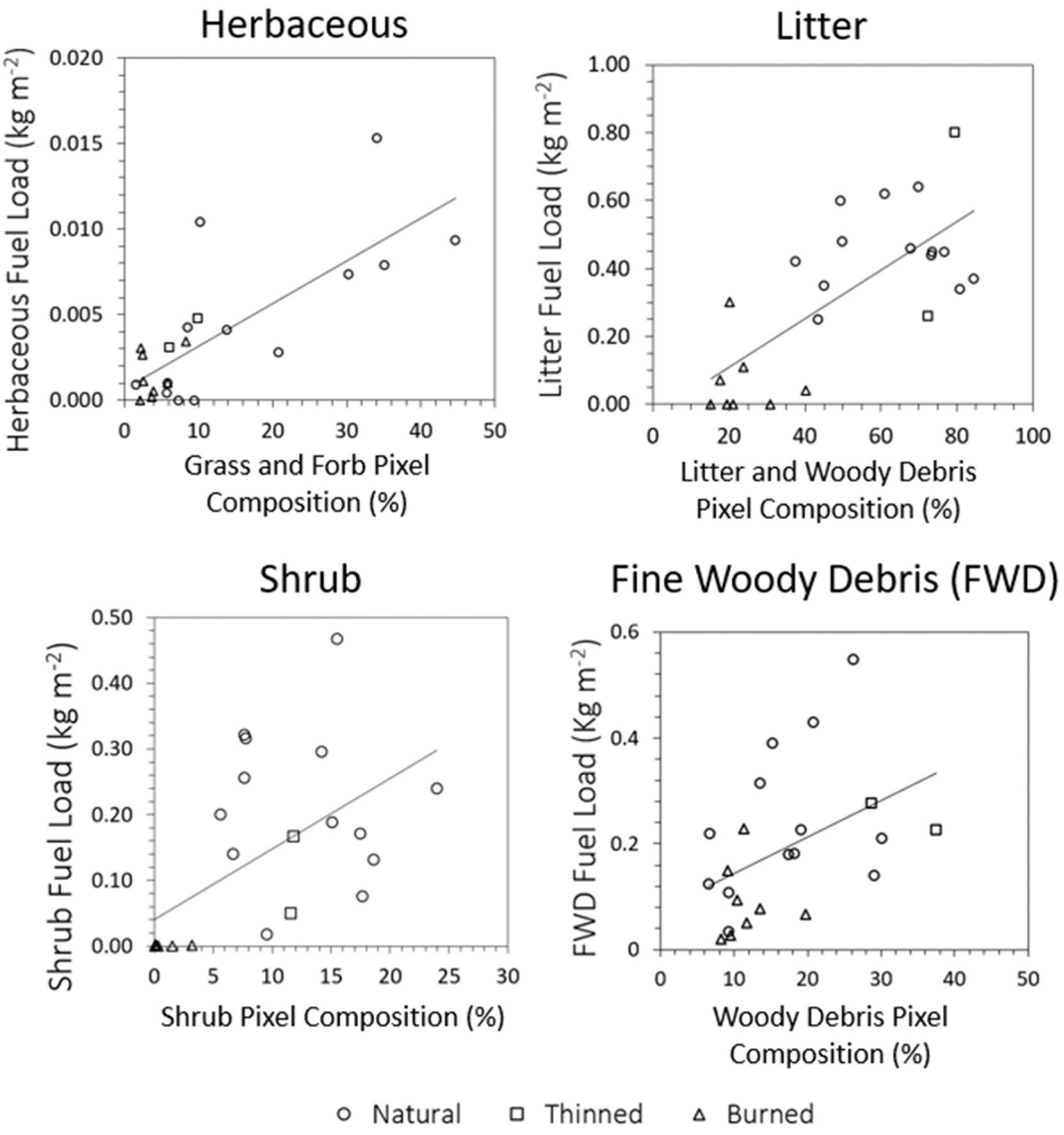

Fig. 6. Relationship between field-measured fuel load and percent cover from pixel composition of manually segmented photos at Pelican Mountain (PM) and Calling Lake (CL) plots, shown for each fuel load category: herbaceous vegetation, litter, shrub, and fine woody debris (FWD).

Table 3
Performance of the semantic segmentation algorithm, by class: mean intersection over union (mIoU), the proportion of overlap between the manually segmented photo and the prediction output; and accuracy, the proportion of pixels in the image that were correctly classified. Test data are from Pelican Mountain (PM) and Calling Lake (CL) field sites.

Class	mIoU	Accuracy
0 - Woody debris	0.462	0.756
1 - Forb	0.333	0.953
2 - Grass	0.49	0.936
3 - Lichen	0.1	0.945
4 - Feather moss	0.283	0.901
5 - Other moss	0.166	0.891
6 - Sphagnum moss	0.74	0.99
7 - non-fuel	0.622	0.987
8 - Shrub	0.396	0.914
9 - Void	0.31	0.748
Average	0.39	0.903

4. Discussion

Nadir photos acquired with smartphones were found to be a viable source of quantitative ground cover information in boreal forest ecosystems. Other studies have reported success using nadir photographs to quantify ground cover or estimate biomass loading (e.g., Abdalla et al., 2019; McCool et al., 2018) but very few have attempted to do so in complex forest environments characterized by multiple discrete cover types. Our first objective was to determine whether nadir photographs acquired in a forested environment could be used to explain field-measured ground cover and above ground biomass values. When photos were manually segmented by cover type, there was a strong ($r >$ 0.84) and statistically significant relationship between estimated percent ground cover from pixel counts of the digital images and corresponding field-measured percent cover of grass, feather moss and sphagnum moss (Table 4). These relationships were weaker but also significant for forb and lichen cover types ($r = 0.69$ for both).

Unsurprisingly, estimates of percent ground cover from manually segmented photos were not strongly correlated with field-measured fuel loads ($r < 0.77$). Nonetheless, our results were still statistically significant and suggest that in situations where rapid, unbiased field sampling

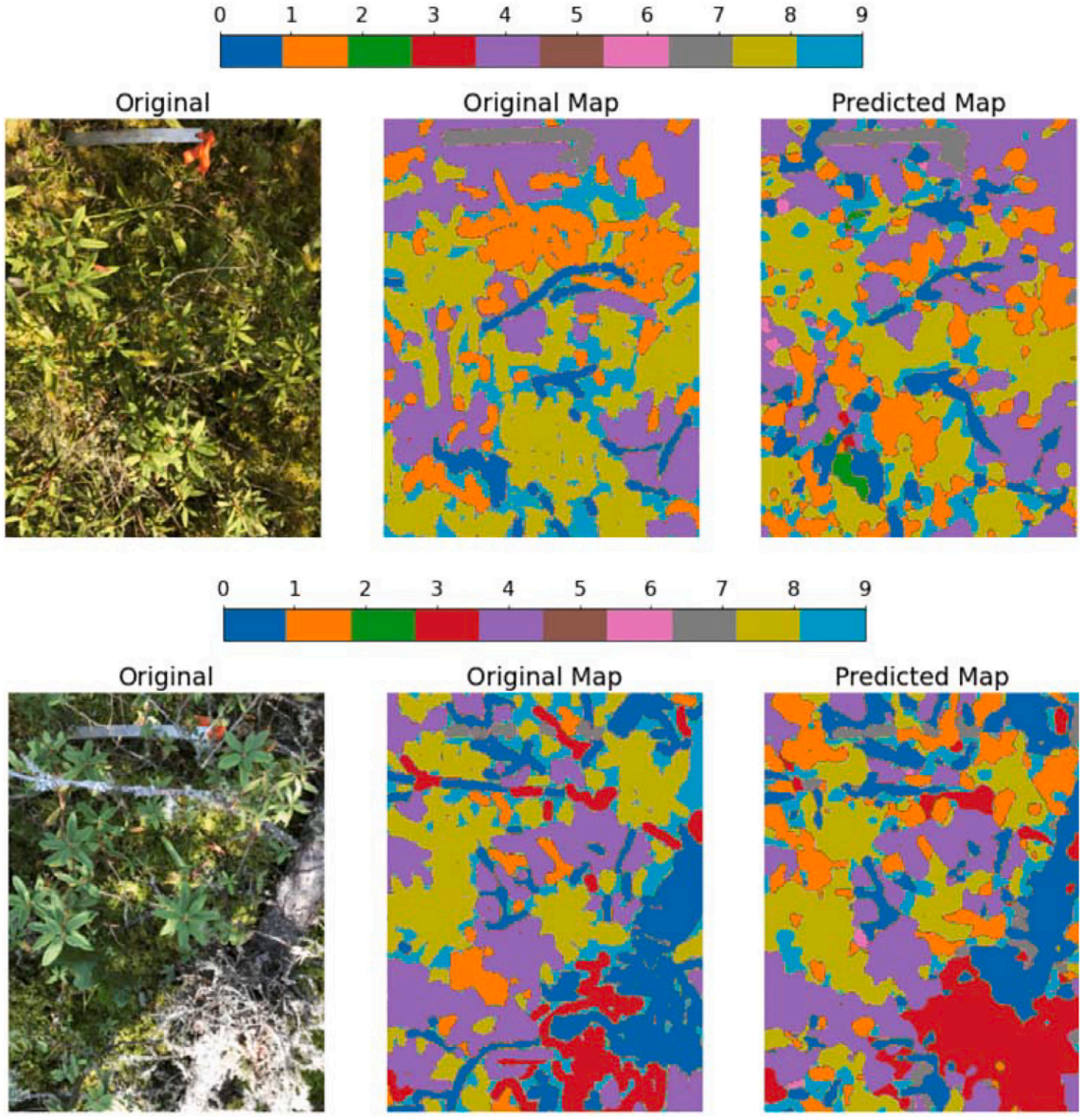

Fig. 7. Samples of raw nadir photographs, manual segmentation and predicted segmentation from our trained deep convolutional neural network.

techniques take priority over more accurate measurements, nadir photographs can adequately describe forest floor attributes. Although promising, segmenting photos manually was labor intensive and therefore costly.

We used our manually segmented photos to train a deep convolutional neural network (DCNN) to perform semantic segmentation. Results indicated that once the network is adequately trained, automatic image segmentation can produce near instant results that are comparable to manual segmentation. Automatic image segmentation has been used successfully in grassland or agricultural settings to detect multiple groundcover types (e.g., Luscier et al., 2006) but detecting and segmenting images is far more difficult in forested environments due to the heterogeneity of vegetation and inconsistent lighting conditions (Macfarlane and Ogden, 2012). When our automatic image segmentation outputs were evaluated with the manually segmented photos on a testing dataset, mIoU values (0.352) were low but accuracies were high (0.950). The low mIoU values were likely due to all classes being equally weighted despite their unequal proportional representation in the photos. Ayhan and Kwan (2020) note that poor classification performance of underrepresented classes, such as lichen and 'other moss' in our study, is due to the deep learning method's loss function, which is biased toward overrepresented classes. This represents a performance barrier for any study using semantic segmentation with few images and high class-imbalance.

In contrast, our high accuracy values indicate the algorithm performed reasonably well. Macfarlane and Ogden (2012) and Salas-Aguilar et al. (2017) are some of the only studies that have used automatically segmented nadir images to estimate understory vegetative cover in forested environments; however, each of these studies performed only binary segmentation (vegetated or non-vegetated). MacFarlane and Ogden's accuracy was 95% and Salas-Aguilar et al. achieved a 94% accuracy. We achieved a similar accuracy (95%) but performed significantly more complex image segmentation by using 10 discrete cover types. Some cover types (e.g. feathermoss and sphagnum moss) are highly similar in appearance yet strong results were achieved using DCNN to perform semantic segmentation. Distinguishing these two moss types is important as they have opposing influences on wildfire behaviour, with feathermoss considered highly flammable and sphagnum moss considered generally resistant to burning due to its characteristic water absorbency (Thompson et al., 2020).

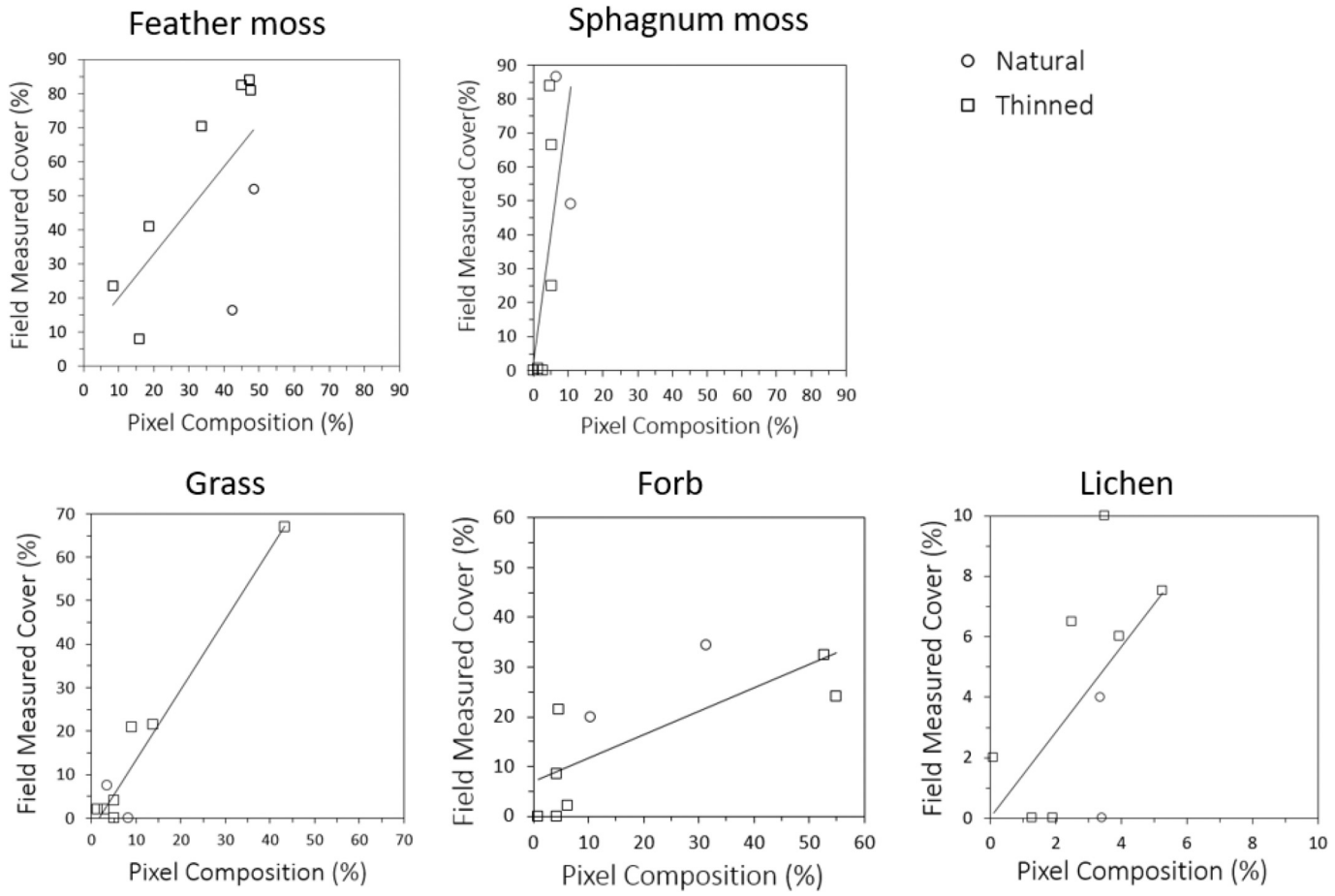

Fig. 8. Field measured percent ground cover for plots at the Conklin (CK) validation site compared with percent cover from pixel composition of photos automatically segmented by trained DCNN, shown for each cover type: feather moss, sphagnum moss, grass, forb, and lichen.

Table 4
Correlations between photo-derived percent cover and field-measured percent cover, by cover type (forb, grass, lichen, feather moss, sphagnum moss) and classification method (manual and algorithm). Asterisk (*) denotes significant correlations ($p < 0.05$).

Cover type	Pearson correlation coefficient (r)	
	Manual image classification PM,CL data	Algorithm-based image classification Independent validation, CK data
Forb	0.69*	0.75*
Grass	0.85*	0.96*
Lichen	0.69*	0.58
Feather moss	0.91*	0.67*
Sphagnum moss	0.88*	0.67*

The final objective of the study was to evaluate the flexibility and robustness of the automated image segmentation algorithm by applying it to a new study site that had similar surface vegetation characteristics. When the automatic image segmentation algorithm was applied to nadir photographs taken at a different geographic location (i.e., CK field site) than those used for training and testing (i.e., PM and CL field sites), the derived percent ground cover values did an adequate job at describing the different field measured ground cover types ($0.58 < r < 0.96$); however, only the forb, grass, feather moss and sphagnum moss cover types were statistically significant ($p < 0.05$), likely due to the small sample size ($n = 9$). Our results are comparable with McCool et al. (2018), one of the few studies that attempted to classify vegetation into grass or forb categories in grassland (i.e., not agriculture) settings. In that study, r values were 0.52–0.82 for grasses and 0.48–0.83 for forbs. Bawden et al. (2017) reported much higher accuracies (96.0% for grasses and 95.9% for forbs) using computer vision-based online detection and classification algorithms, but their study was performed in a much simpler monoculture crop and was only used for weed detection.

Overall, ground cover measurements derived from manually segmented images exhibited a stronger correlation with field measurements compared with ground cover measurements derived from automatically segmented photos. This may indicate that the deep learning algorithm struggled to adapt to slightly different forest floor structures than those used for training. Based on Pearson correlations (r), automatic image classification actually outperformed manual classification when comparing forb and grass cover measurements from photos to corresponding field-based measurements, but this is likely due to the influence of outliers. It is noteworthy that the algorithm was trained with a small set of images ($n = 290$), which necessitated the use of data augmentation strategies to increase the number of training images, but likely at the cost of reduced flexibility and robustness for applying the trained network in new situations. We expect that training the network with a larger set of images taken at different sites would greatly improve the algorithm's performance in new locations.

Regardless of whether nadir photos are manually or automatically segmented, these images are inherently limited by their two-dimensional representation of ground cover types that exhibit complex three-dimensional structures in reality. Field measurements are designed to detect and inventory vertically layered surface cover types, whereas nadir photographs contain a simplified two-dimensional representation of these layers as viewed from above. Nonetheless, strong

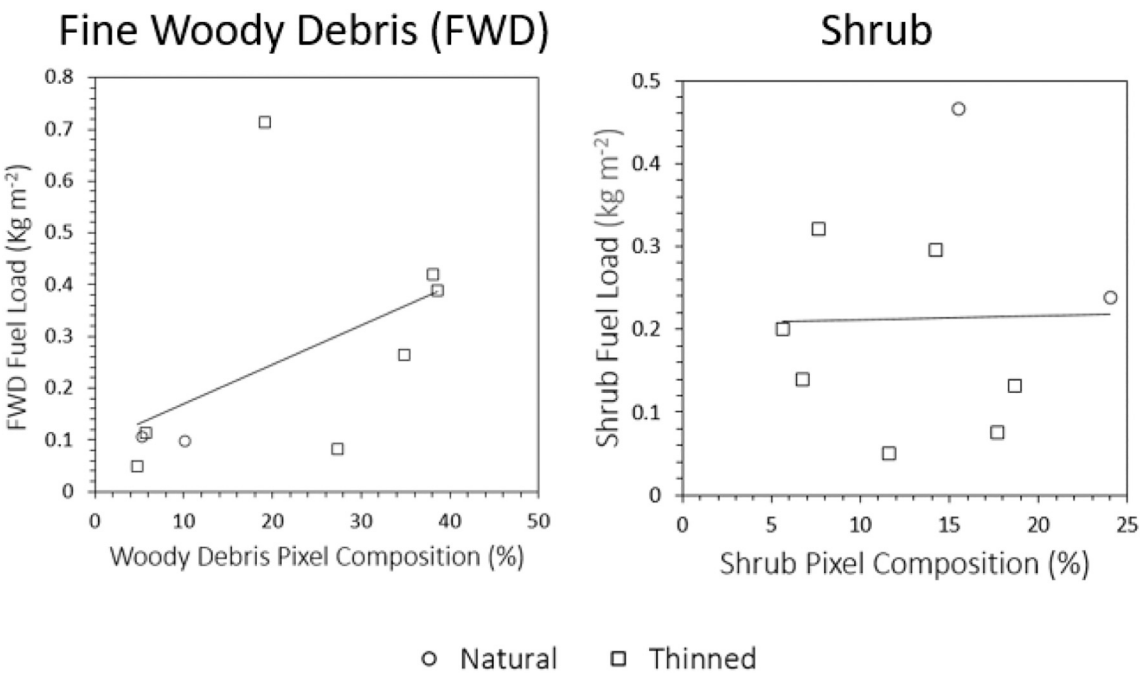

Fig. 9. Field measured fuel load values for plots at the Conklin (CK) validation site compared with pixel composition of photos automatically segmented by trained DCNN; shown for two fuel load categories: fine woody debris (FWD) and shrub.

Table 5
Correlations between photo-derived percent cover and field-measured fuel load, by cover type (fine woody debris, shrub, herbaceous, litter) and classification method (manual and algorithm). Asterisk (*) denotes significant correlations ($p < 0.05$).

Cover type	Pearson correlation coefficient	
	Manual image classification PM, CL data ($n = 23$)	Algorithm-based image classification Independent validation, CK data ($n = 9$)
Fine woody debris	0.42*	0.50
Shrub	0.57*	0.02
Herbaceous	0.77*	NA
Litter	0.72*	NA

correlations between field measurements of percent ground cover and corresponding estimates from image pixel counts suggest the simplified representations of ground cover composition in nadir photographs may indeed be useful for rapid measurement in field settings.

Although the results of this study are encouraging, multiple sources of error are expected to affect some of the results. Human error during field measurements, the use of allometric equations to calculate fuel load values, human error in segmenting the nadir photographs into cover type categories, and the relatively low number of images available for training the semantic segmentation DCNN all likely played a role in some of the variability observed within the data. The relaxed protocol that we used for acquiring nadir photographs is not expected to introduce significant bias or differences in percent cover calculations, given that cover estimates were calculated as proportions rather than area measurements.

Future work would benefit from using larger photo datasets when training the automatic semantic segmentation algorithm, which may increase its accuracy when applying the algorithm to new locations. Multi-lens cameras now standard on consumer-grade smartphones could be used to sense depth in the scene and help the semantic segmentation address the influence of overlapping vegetation. Image metadata such as exposure settings could potentially be used to standardize images and enable distributed data collection of nadir photographs by groups of personnel working at different times of the day and using different brands of smartphones. Future work could also explore techniques such as active learning and pre-training on new semantically related datasets.

Potential long-term implications of this research include eventual development of a smartphone-based app to quickly and automatically estimate percent ground cover and surface biomass loadings in forest ecosystems. In recent years, smartphone applications have enabled the public to contribute to data collection and participate in citizen science programs (e.g. iNaturalist, NoiseTube, Secchi). With crowd-sourcing, ground cover observations can be collected in quantities that far exceed those of research programs that rely solely on trained professionals and field crews (Ferster and Coops, 2014; Van Horn et al., 2018).

Apps have been developed to collect forest structure information, but data accuracy can vary depending on whether a forestry professional or non-professional conducts the observation (Ferster and Coops, 2014). By using an automated algorithm to process nadir photographs taken with a flexible protocol, inconsistencies between professional and non-professional observations are eliminated. The wide-ranging geospatial data that could be collected with the help of the public could be especially useful for ecological studies that rely on ground cover information (e.g. Booth et al., 2006; Brewer, 2016; Silva et al., 2010). With additional research, pixel count to biomass relationships could potentially be used to generate surface fuel load inputs required to predict fire behaviour in models such as CanFIRE (de Groot, 2012) and FIRETEC (Linn, 1997), as well as the Byram (1959) and Rothermel (1972) fire spread models, which are used to inform mitigation and response decisions. Overall, results of this study suggest there is considerable promise for using smartphone technology to quickly document surface vegetation relevant to a wide range of ecological, forestry, and wildfire related objectives.

Author contributions

H.C. conducted the statistical analysis and led the drafting of the manuscript, with writing contributions from all authors. J.B.

conceptualized the study, developed the photo acquisition protocol, and oversaw analysis of field-based measurements in relation to cover estimated from manual and automatically classified images. P.P. researched the choice of DCNN architecture, performed implementation and training of the chosen approach, and ran the resulting system, with input and oversight from M.B.

Declaration of Competing Interest

The authors declare no conflict of interest.

Acknowledgements

This research was funded by Alberta Agriculture, Forestry and Rural Economic Development (AAFRED) through the Canadian Partnership for Wildland Fire Science, grant agreement number 18GRWMB06. We thank AAFRED field crews for assistance with data collection; A. Sharma for assistance manually processing nadir photographs; J. Randall for contributions to literature review; and B. Finch for computing systems support.

References

Abdalla, A., Cen, H., Wan, L., Rashid, R., Weng, H., Zhou, W., He, Y., 2019. Fine-tuning convolutional neural network with transfer learning for semantic segmentation of ground-level oilseed rape images in a field with high weed pressure. Comput. Electron. Agric. 167, 105091.

Ayhan, B., Kwan, C., 2020. Tree, shrub, and grass classification using only RGB images. Remote Sens. 12, 1333.

Bawden, O., Kulk, J., Russell, R., McCool, C., English, A., Dayoub, F., Lehnert, C., Perez, T., 2017. Robot for weed species plant-specific management. J. Field Robotics 34 (6), 1179–1199.

Bessie, W.C., Johnson, E.A., 1995. The relative importance of fuels and weather on fire behavior in subalpine forests. Ecology 76, 747–762.

Beverly, J.L., Wotton, B.M., 2007. Modelling the probability of sustained flaming: predictive value of fire weather index components compared with observations of site weather and fuel moisture conditions. Int. J. Wildland Fire 16 (2), 161–173.

Bonham, C.D., 1989. Measurements for Terrestrial Vegetation. John Wiley & Sons, New York.

Booth, D.T., Cox, S.E., Fifield, C., Phillips, M., Williamson, N., 2005. Image analysis compared with other methods for measuring ground cover. Arid Land Res. Manag. 19 (2), 91–100.

Booth, D.T., Cox, S.E., Meikle, T.W., Fitzgerald, C., 2006. The accuracy of ground-cover measurements. Rangel. Ecol. Manag. 59 (2), 179–188.

Breheret, Amaury, 2017. Pixel Annotation Tool. http://github.com/abreheret/PixelAnnotationTool.

Brewer, J.S., 2016. Natural canopy damage and the ecological restoration of fire-indicative groundcover vegetation in an oak-pine forest. Fire Ecology 12 (2), 105–126.

Brown, J.K., 1974. Handbook for inventorying downed woody material. *Gen. Tech. Rep. INT-16. Ogden, UT: US Department of Agriculture, Forest Service, intermountain Forest and range Experiment Station. 24 p., 16*.

Byram, G.M., 1959. Combustion of forest fuels. In: Davis, K.P. (Ed.), Forest Fire: Control and Use. McGraw-Hill, New York, NY, USA, pp. 61–89.

Chen, L.-C., Papandreou, G., Schroff, F., Adam, H., 2017. Rethinking atrous convolution for semantic image segmentation. arXiv preprint. https://doi.org/10.48550/arXiv.1706.05587. arXiv:1706.05587.

Chianucci, F., 2020. An overview of in situ digital canopy photography in forestry. Can. J. For. Res. 50 (3), 227–242.

de Groot, B., 2012. CANFIRE Canadian Fire Effects Model. In: *Natural Resources Canada Canadian Forest Service–Great Lakes Forestry Centre*. Frontline Express, Bulletin, p. 62.

Delisle, G.P., Woodard, P.M., 1988. Constants for calculating fuel loads in Alberta. Forest Management Note No. 45. Northern Forestry Centre: Edmonton, Alberta.

Duan, T., Zheng, B., Guo, W., Ninomiya, S., Guo, Y., Chapman, S.C., 2017. Comparison of ground cover estimates from experiment plots in cotton, sorghum and sugarcane based on images and ortho-mosaics captured by UAV. Funct. Plant Biol. 44 (1), 169–183.

Eigen, D., Fergus, R., 2015. Predicting depth, surface normals and semantic labels with a common multi-scale convolutional architecture. In: Proceedings of the 2015 IEEE international conference on computer vision, pp. 2650–2658, Santiago, Chile, December 2015.

Etchberger, R.C., Krausman, P.R., Mazaika, R., 1989. Mountain sheep habitat characteristics in the Pusch ridge wilderness, Arizona. J. Wildl. Manag. 902–907.

Everingham, M., Van Gool, L., Williams, C.K.I., Winn, J., Zisserman, A., 2010. The PASCAL visual object classes (VOC) challenge. Int. J. Comput. Vis. 88 (2), 303–338.

Ferster, C.J., Coops, N.C., 2014. Assessing the quality of forest fuel loading data collected using public participation methods and smartphones. Int. J. Wildland Fire 23 (4), 585–590.

Ferster, C.J., Coops, N.C., Harshaw, H.W., Kozak, R.A., Meitner, M.J., 2013. An exploratory assessment of a smartphone application for public participation in forest fuels measurement in the wildland-urban interface. Forests 4 (4), 1199–1219.

Graham, R.T., McCaffrey, S., Jain, T.B., 2004. Science Basis for Changing Forest Structure to Modify Wildfire Behavior and Severity Gen. Tech. Rep. RMRS-GTR-120 Fort Collins, CO: U.S. United States Department of Agriculture Forest Service, Rocky Mountain Research Station, p. 43.

Hahn, I., Scheuring, I., 2003. The effect of measurement scales on estimating vegetation cover: a computer-assisted experiment. Community Ecol. 4 (1), 29–33.

Houghton, R.A., Hall, F., Goetz, S.J., 2009. Importance of biomass in the global carbon cycle. J. Geophys. Res. Biogeosci. 114 (G2).

Keane, R.E., Dickinson, L.J., 2007. Development and Evaluation of the Photoload Sampling Technique. In: Research Paper RMRS-RP-61. Fort Collins, CO: U.S. Department of Agriculture, Forest Service, Rocky Mountain Research Station, p. 29.

Keane, R.E., Gray, K., 2013. Comparing three sampling techniques for estimating fine woody down dead biomass. Int. J. Wildland Fire 22 (8), 1093–1107.

Kennedy, K.A., Addison, P.A., 1987. Some considerations for the use of visual estimates of plant cover in biomonitoring. J. Ecol. 151–157.

Kingma, D.P., Ba, J., 2014. Adam: a method for stochastic optimization. arXiv preprint. https://doi.org/10.48550/arXiv.1412.6980 arXiv:1412.6980.

Lin, T.-Y., Maire, M., Belongie, S., Bourdev, L., Girshick, R., Hays, J., Perona, P., Ramanan, D., Zitnick, C.L., Dollar, P., 2015. Microsoft COCO: Common Objects in Context. arXiv preprint arXiv 1405.0312.

Linn, R., 1997. A Transport Model for Prediction of Wildfire Behavior, vols. No. LA-13334-T. Los Alamos National Lab, NM (United States).

Luscier, J.D., Thompson, W.L., Wilson, J.M., Gorham, B.E., Dragut, L.D., 2006. Using digital photographs and object-based image analysis to estimate percent ground cover in vegetation plots. Front. Ecol. Environ. 4 (8), 408–413.

Lutes, D.C., Keane, R.E., Caratti, J.F., Key, C.H., Benson, N.C., Sutherland, S., Gangi, L.J., 2005. *FIREMON: Fire Effects Monitoring and Inventory System*. Gen. Tech. Rep. RMRS-GTR-XXX-CD. Ogden UT: U.S. Department of Agriculture, Forest Service, Rocky Mountain Research Station.

Macfarlane, C., Ogden, G.N., 2012. Automated estimation of foliage cover in forest understorey from digital nadir images. Methods Ecol. Evol. 3 (2), 405–415.

McCool, C., Beattie, J., Milford, M., Bakker, J.D., Moore, J.L., Firn, J., 2018. Automating analysis of vegetation with computer vision: cover estimates and classification. Ecology and evolution 8 (12), 6005–6015.

McRae, D.J., Alexander, M.E., Stocks, B.J., 1979. Measurement and Description of Fuels and Fire Behavior on Prescribed Burns: A Handbook. Department of the Environment, Canadian Forestry Service, Great Lakes Forest Research Centre.

Michener, W.K., Houhoulis, P.F., 1997. Detection of vegetation changes associated with extensive flooding in a forested ecosystem. Photogramm. Eng. Remote. Sens. 63 (12), 1363–1374.

Morrison, L.W., 2016. Observer error in vegetation surveys: a review. J. Plant Ecol. 9 (4), 367–379.

Nalder, I.A., Wein, R.W., Alexander, M.E., de Groot, W.J., 1999. Physical properties of dead and downed round-wood fuels in the boreal forests of western and northern Canada. Int. J. Wildland Fire 9, 85–99.

Olson, C.M., Martin, R.E., 1981. Estimating biomass of shrubs and forbs in Central Washington Douglas-fir stands. Res. Note PNW-RN-380. Portland, OR: U.S. Department of Agriculture, Forest Service. Pacific Northwest Forest and Range Experiment Station. 6 p.

Patrignani, A., Ochsner, T.E., 2015. Canopeo: a powerful new tool for measuring fractional green canopy cover. Agron. J. 107 (6), 2312–2320.

Pyke, D.A., Herrick, J.E., Shaver, P., Pellant, M., 2002. Rangeland health attributes and indicators for qualitative assessment. Rangeland Ecol. & Manag./J. Range Manag. Archiv. 55 (6), 584–597.

R Core Team, 2020. R: A Language and Environment for Statistical Computing. R Foundation for Statistical Computing, Vienna, Austria http://www.R-project.org/.

Rosset, C., Brand, R., Caillard, I., Fiedler, U., Gollut, C., Schmocker, A., Weber, D., Wuillemin, E., 2014. *MOTI: L'inventaire forestier facilité par le smartphone* Haute École Spécialisée Bernoise BFH, Haute École des Sciences Agronomiques, Forestières et Alimentaires HAFL. Division Sciences Forestières.

Rothermel, R.C., 1972. A mathematical model for predicting fire spread in wildland fuels. Res. Pap. INT115. Ogden, UT: U.S. Department of Agriculture, Forest Service. Intermountain Forest and Range Experiment Station, 40 p.

Rouvinen, T., 2014. Trestima—digital photographs for Forest inventory. Sibirskij Lesnoj Žurnal (Siberian J. For. Sci.) 1, 69–76.

Salas-Aguilar, V., Sánchez-Sánchez, C., Rojas-García, F., Paz-Pellat, F., Valdez-Lazalde, J. R., Pinedo-Alvarez, C., 2017. Estimation of vegetation cover using digital photography in a regional survey of Central Mexico. Forests 8 (10), 392.

Sikkink, P.G., Keane, R.E., 2008. A comparison of five sampling techniques to estimate surface fuel loading in montane forests. Int. J. Wildland Fire 17 (3), 363–379.

Silva, E.B., Franco, J.C., Vasconcelos, T., Branco, M., 2010. Effect of ground cover vegetation on the abundance and diversity of beneficial arthropods in citrus orchards. Bull. Entomol. Res. 100 (4), 489.

Song, W., Mu, X., Yan, G., Huang, S., 2015. Extracting the green fractional vegetation cover from digital images using a shadow-resistant algorithm (SHAR-LABFVC). Remote Sens. 7 (8), 10425–10443.

Spurr, J.M., Barnes, B.V., 1973. Forest Ecology, Second edition, 575. Ronald Press, New York, New York.

Sykes, J.M., Horrill, A.D., Mountford, M.D., 1983. Use of visual cover assessments as quantitative estimators of some British woodland taxa. J. Ecol. 437–450.

Thompson, D.K., Schroeder, D., Wilkinson, S.L., Barber, Q., Baxter, G., Cameron, H., Rodell, C., 2020. Recent crown thinning in a boreal black spruce forest does not

reduce spread rate nor total fuel consumption: results from an experimental crown fire in Alberta. Canada. Fire 3 (3), 28.
Tobler, W.R., 1970. A computer movie simulating urban growth in the Detroit region. Econ. Geogr. 46, 234–240.
Urbanek, Simon, 2013. Png: read and write PNG images. R package version 0, 1–7. http://CRAN.R-Project.org/package=png.
Van Horn, G., Mac Aodha, O., Song, Y., Cui, Y., Sun, C., Shepard, A., Belongie, S., 2018. The inaturalist species classification and detection dataset. In: Proceedings of the 2018 IEEE/CVF Conference on Computer Vision and Pattern Recognition, pp. 8769–8778.
Van Wagner, C.E., 1968. The line intersect method in forest fuel sampling. For. Sci. 14 (1), 20–26.
Vastaranta, M., Latorre, E.G., Luoma, V., Saarinen, N., Holopainen, M., Hyyppä, J., 2015. Evaluation of a smartphone app for forest sample plot measurements. Forests 6 (4), 1179–1194.
Volkova, L., Sullivan, A.L., Roxburgh, S.H., Weston, C.J., 2016. Visual assessments of fuel loads are poorly related to destructively sampled fuel loads in eucalypt forests. Int. J. Wildland Fire 25 (11), 1193–1201.
Warren, W.G., Olsen, P.F., 1964. A line intersect technique for assessing logging waste. For. Sci. 10 (3), 267–276.
Whitman, E., Parisien, M.A., Thompson, D.K., Flannigan, M.D., 2019. Short-interval wildfire and drought overwhelm boreal forest resilience. Sci. Rep. 9 (1), 1–12.
Wickham, H., 2016. ggplot2: Elegant Graphics for Data Analysis. Springer-Verlag, New York.
Yu, X., Guo, X., 2021. Extracting fractional vegetation cover from digital photographs: a comparison of in situ, SamplePoint, and image classification methods. Sensors 21, 7310.